Three-dimensional "Mercedes-Benz" model for water

Cite as: J. Chem. Phys. **131**, 054505 (2009); https://doi.org/10.1063/1.3183935
Submitted: 12 February 2009 . Accepted: 30 June 2009 . Published Online: 06 August 2009

Cristiano L. Dias, Tapio Ala-Nissila, Martin Grant, and Mikko Karttunen

Three-dimensional "Mercedes-Benz" model for water

Cristiano L. Dias,[1,a)] Tapio Ala-Nissila,[2,3,b)] Martin Grant,[4,c)] and Mikko Karttunen[1,d)]
[1]*Department of Applied Mathematics, The University of Western Ontario, London, Ontario N6A 5B7, Canada*
[2]*Department of Physics, Brown University, Providence Rhode Island 02912-1 843, USA*
[3]*Department of Applied Physics and COMP Center of Excellence, Helsinki University of Technology, P.O. Box 1100, FI-02015 TKK Espoo, Finland*
[4]*Department of Physics, McGill University, 3600 rue University, Montréal, Québec H3A 2T8, Canada*

(Received 12 February 2009; accepted 30 June 2009; published online 6 August 2009)

In this paper we introduce a three-dimensional version of the Mercedes-Benz model to describe water molecules. In this model van der Waals interactions and hydrogen bonds are given explicitly through a Lennard-Jones potential and a Gaussian orientation-dependent terms, respectively. At low temperature the model freezes forming Ice-I and it reproduces the main peaks of the experimental radial distribution function of water. In addition to these structural properties, the model also captures the thermodynamical anomalies of water: The anomalous density profile, the negative thermal expansivity, the large heat capacity, and the minimum in the isothermal compressibility.
 [DOI: 10.1063/1.3183935]

I. INTRODUCTION

Water is the most important fluid on earth. It covers two-thirds of the planet's surface and controls its climate. Most importantly, water is necessary for carbon-based organic life being the solvent in most *in vivo* chemical reactions. Its unique hydration properties drive biological macromolecules toward their three-dimensional (3D) structure, thus accounting for their function in living organisms.[1] Water exhibits anomalous properties that affect life at a larger scale. For example, mammals benefit from the large latent heat of water to cool them down through sweating, while water's large heat capacity prevents local temperature fluctuations, facilitating thermal regulation of organisms.

These anomalous properties result from a competition between isotropic van der Waals interactions and highly directional hydrogen bonding (H-bond). A large number of models of varying complexity have been developed and analyzed to model water's extraordinary properties, for reviews, see, e.g., Refs. 2–5, but none of the current models can correctly reproduce all physical properties of water. Those models are typically calibrated against experimental data, for example, the radial distribution function (RDF) at ambient conditions,[6,7] or the temperature of maximum density,[8] i.e., $T=3.98$ °C. While there is no guarantee that a model optimized to reproduce a given property is able to account for others, adding details increases its quantitative accuracy. For example, TIP5P, which describes water through five interacting sites, is typically more accurate[8] than models with three or four interacting sites. The addition of each interacting site, however, makes the model considerably more demanding computationally. This is an undesirable feature since a large number of water molecules is required to hydrate even the smallest peptides resulting in a high computational cost. Thus, simple models, such as SPC (Ref. 9) and TIP3P,[2,10] are the most used ones in computational studies of biologically motivated systems. In addition, new models and improvements appear frequently in literature, see, e.g., Refs. 11–15, and references in them.

Coarse-grained models have also been developed and used to study the emergence of water's anomalous properties from its atomic constituents. Both lattice[16–18] and continuous models[19–22] have been applied. Current coarse-grained models cannot, however, be easily used to study hydration of macromolecules, because they cannot reproduce the structure of liquid water which is essential in studies of biological systems and molecules.[1] A proper structural description is required since hydration and, in particular, the hydrophobic effect, which is the main driving force for protein folding,[23,24] depend on the amount of structural order close to the hydrated molecule versus the amount of order in bulk water. A simplified model that would account for both thermodynamical and structural properties of water, would therefore be highly beneficial in studies related to the hydrophobic effect, protein folding and macromolecules in general.

The main purpose of this work is to introduce a simple but realistic model that reproduces both the main structural and thermodynamic properties of water. To this end, we extend the two dimensional (2D) Mercedes-Benz (MB) model[25] to 3D. In 2D, the MB model has already provided insights into several properties of water: Its anomalous thermodynamical behavior,[19] hydration of nonpolar solutes,[26] ion solvation,[27] cold denaturation of proteins,[28] and the properties of different amino acids.[29] Despite this success, there are several mechanisms which cannot be studied in two dimensions and an extension to 3D is needed.

We show that a previously proposed framework for the 3D MB model[30,31] does not reproduce the thermodynamical anomalies of water. Here, we extend the model to overcome that problem by making H-bonding dependent on the local

[a)]Electronic mail: diasc@physics.mcgill.ca.
[b)]Electronic mail: tapio.ala-nissila@tkk.fi.
[c)]Electronic mail: martin.grant@mcgill.ca.
[d)]Electronic mail: mkarttu@uwo.ca.

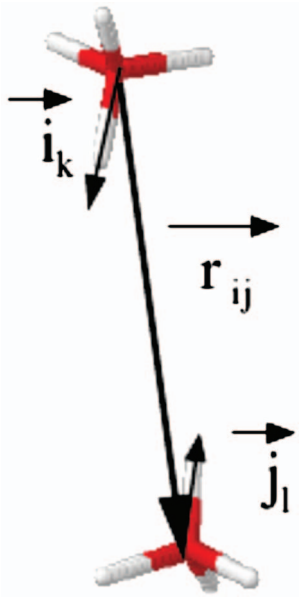

FIG. 1. Schematic representation of two MB molecules and important vectors defining their interaction.

environment of atoms by penalizing compact configurations in favor of open-packed ones. With this implementation, structural and thermodynamical properties are recovered qualitatively. We would like to emphasize that the aim of the present model is to provide structural information on water but not to faithfully reproduce all of the properties of this material. Thus the model is not intended to replace atomistically accurate models, such as TIP5P, but rather as an improved statistical mechanics model for water.

The rest of this paper is organized as follows: Next, we introduce and discuss the existing 3D MB model, and propose a correction that makes the model suitable to describe thermodynamical and structural properties of water. In the same section, we present the Monte Carlo scheme and the cooling protocol used in this work. In the section entitled results, experimental data are compared qualitatively to our simulations. Finally, we present our conclusions and a discussion in Sec. IV.

II. THE MODEL

A. Mercedes Benz model

In the 3D MB model,[30] water molecules interact explicitly through two types of empirical potentials: H-bonds and van der Waals. H-bonds are directional and account for the tetrahedral structure of water which is described by four arms separated from each other by angles of 109.47°, see Fig. 1. The energy of H-bonds is minimized whenever arms of adjacent molecules point toward each other. Mathematically if $\vec{X}_i$ represents the position of the ith particle and its four unitary arms, which are denoted by $\vec{i}_k$ (with $k=1,2,3,4$), then H-bond interaction between molecules i and j can be written as

$$U_{\mathrm{HB}}(\vec{X}_i,\vec{X}_j)=\sum_{k,l=1}^{4} U_{\mathrm{HB}}^{kl}(r_{ij},\vec{i}_k,\vec{j}_l), \tag{1}$$

where

$$U_{\mathrm{HB}}^{kl}(r_{ij},\vec{i}_k,\vec{i}_l)=\epsilon_{\mathrm{HB}}G(r_{ij}-R_{\mathrm{HB}},\sigma_R) \times G(\vec{i}_k\hat{r}_{ij}-1,\sigma_\theta)G(\vec{j}_l\hat{r}_{ij}+1,\sigma_\theta) \tag{2}$$

and $G(x,\sigma)$ is an un-normalized Gaussian function

$$G(x,\sigma)=\exp[-x^2/2\sigma^2]. \tag{3}$$

The above mathematical description ensures that the intensity of a H-bond is maximized whenever the arms of neighboring molecules are aligned with the vector $\vec{r_{ij}}$ joining their centers of mass and whenever their distance is equal to R_{HB}.

The spherically symmetric van der Waals interactions are approximated by a Lennard-Jones potential:

$$U_{\mathrm{LJ}}(r_{ij})=4\epsilon_{\mathrm{LJ}}\left[\left(\frac{\sigma_{\mathrm{LJ}}}{r_{ij}}\right)^{12}-\left(\frac{\sigma_{\mathrm{LJ}}}{r_{ij}}\right)^{6}\right], \tag{4}$$

where ϵ_{LJ} describes the strength of the interaction and σ_{LJ} is the particle diameter. Then, the total energy describing two MB particles is given by

$$U(\vec{X}_i,\vec{X}_j)=U_{\mathrm{LJ}}(r_{ij})+U_{\mathrm{HB}}(\vec{X}_i,\vec{X}_j). \tag{5}$$

Bizjak *et al.*[31] studied this model using the following set of parameters: $\epsilon_{\mathrm{HB}}=-1$, $\epsilon_{\mathrm{LJ}}=1/35\epsilon_{\mathrm{HB}}$, $R_{\mathrm{HB}}=1$, $\sigma_{\mathrm{LJ}}=0.7R_{\mathrm{HB}}$, and $\sigma_R=\sigma_\theta=0.085$. They assumed a diamond structure for the model's ground state which is the configuration taken by oxygen atoms when water forms cubic-ice, i.e., Ice-I_c. When tested against simulation, however, this assumption fails and the system solidifies in configurations which are much more compact than Ice-I. This is shown in Fig. 2(a) where the system assumes densities of about 2 g/cm^3 at different temperatures,[32] much beyond the density of water ($\sim$1 g/cm^3). As a result, the model does not reproduce the structure of liquid water as can be seen from the RDF in the inset of Fig. 2(a). The simulated RDF has a nonrealistic peak at a distance corresponding to the van der Waals radius.

To remove the unwanted first peak of the RDF, one can set $\sigma_{\mathrm{LJ}}=2^{-1/6}$. However, even in this case the density of the system is much larger than the density of real water and the system solidifies in a perfect Ice-VII configuration: Two interpenetrating diamond lattices with no H-bonds connecting these lattices. Ice-VII appears to be the optimized ground state for systems trying to maximize their density within a tetrahedral symmetry. It is therefore natural that the original 3D MB model with $\sigma_{\mathrm{LJ}}=2^{-1/6}$, whose H-bond term imposes a tetrahedral configuration and the van der Waals term favors compact conformations, has this structure as its ground state. This preference for Ice-VII is shown in Fig. 2(b) where we show the average density obtained along cooling a system of 256 MB particles. Each temperature shown in this figure was obtained by equilibrating the system for 5×10^4 time steps and gathering statistics for the same amount of time. The density of the solid phase is found to be $\sim$1.65 g/cm^3 which is close to experimental density of Ice-VII. In the inset of this figure we show the Ice-VII structure obtained from the

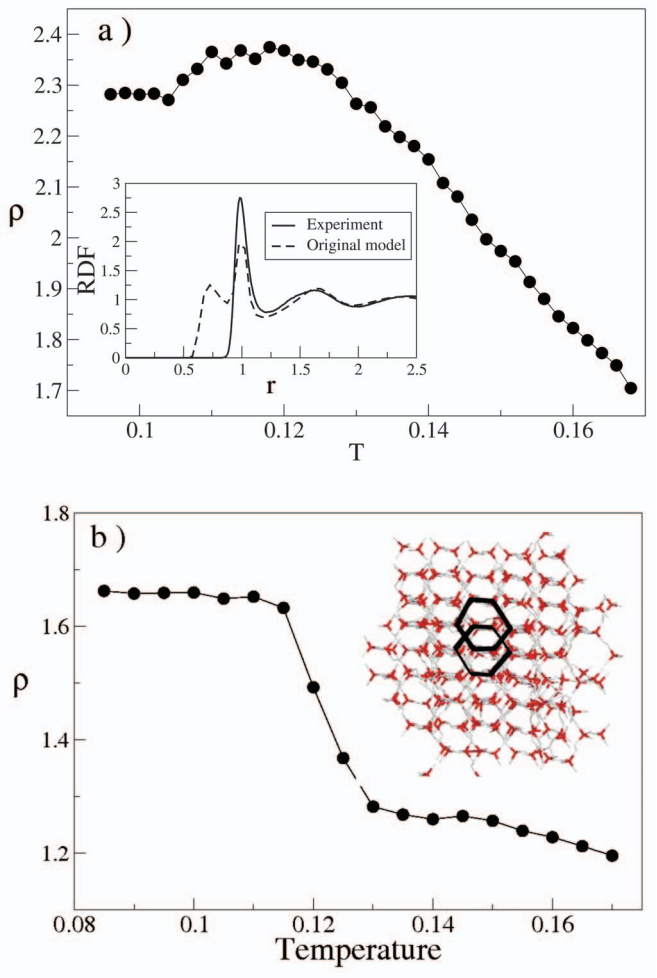

FIG. 2. (a) Dependence of the density (in g/cm^3) on temperature for the original MB model with $\sigma_{LJ}=0.7$ at $P=0.12$. In the inset we compare the radial distribution function at $T=0.14$ with experiment at $T=298$ K. (b) Dependence of the density (in g/cm^3) on temperature for the original MB model with $\sigma_{LJ}=2^{-1/6}$ and $P=0.12$. In inset we show the structure that corresponds to the solid phase of the model: Ice-VII. As a guide to the eye two hexagons representing the two interpenetrating diamond structure of Ice-VII are drawn.

quenching. Notice that Ice-VII is not the desired ground state for models of water at ambient pressure such that 3D lattice models for this material have an explicit energetic term penalizing compact configurations of this type.[18,33,34]

Despite the problems cited above, the 3D MB model remains an attractive coarse-grained model for water. It does not require calculation of charges, which enables longer simulation times desperately needed in studies of macromolecules. It also holds the promise of being able to provide a qualitatively accurate description of the structure of water due to its tetrahedral nature[35] and water's thermodynamical properties since the model exhibits both open and close packed structures required to described water's anomalous behavior.[20] Next, we describe how the original MB model can be improved to better describe the structure and thermodynamics of water.

B. Corrections to the Mercedes-Benz model

To resolve the above problems, we introduce a term that depends on the local environment of particles. Our approach is inspired by Tersoff-like potentials for covalent materials.[36] This term penalizes H-bonds which are formed in crowded environments through the factor

$$b(z_i)=\begin{cases}1, & \text{if } z_i\le 4;\\ \left(\dfrac{4}{z_i}\right)^{\nu}, & \text{if } z_i>4,\end{cases} \tag{6}$$

where z_i is the coordination of atom i, computed as $z_i=\Sigma_{k\neq i}f(r_{ik})$ with the cutoff function defined by[36]

$$f(r_{ij})=\begin{cases}1, & r<R-D;\\ \dfrac{1}{2}-\dfrac{1}{2}\sin\left(\dfrac{\pi}{2}(r-R)/D\right), & R-D<r<R+D;\\ 0, & r>R+D,\end{cases} \tag{7}$$

where R and D are chosen as to include the first-neighbor shell only. Note that $f(r)$ decreases continuously from 1 to 0 in the range $R-D<r<R+D$.

The energy of H-bonds corrected through Eq. (6) becomes

$$U^c_{\mathrm{HB}}(\vec{X}_i,\vec{X}_j)=b(z_i)\sum_{k,l=1}^{4}U^{kl}_{\mathrm{HB}}(r_{ij},\vec{i}_k,\vec{j}_l). \tag{8}$$

This equation penalizes H-bonds whenever interacting molecules have more than four neighbors. This inhibits the formation of compact tetrahedral phases, e.g., Ice-VII, and favors open-packed tetrahedral phases such as Ice-I.

In order to ensure that H-bonds favor chairlike configurations required for diamond structure, we also add a standard potential with threefold symmetry for dihedral angles. This potential adds an energetic cost to the H-bond between arm m of molecule i and arm n of molecules j, if the dihedral angle formed by the other arms of these molecules is not 60°:

$$U^{mn}_{\phi}(\vec{X}_i,\vec{X}_j)=\frac{-\epsilon_{\phi}}{2}U^{mn}_{\mathrm{HB}}(r_{ij},\vec{i}_m,\vec{j}_n)b(z_i)\sum_{\substack{k\neq m\\ l\neq n}}(1+\cos(3\phi_{kl})), \tag{9}$$

where ϵ_{ϕ} is the strength of the interaction. The term $U^{mn}_{\mathrm{HB}}(r_{ij},\vec{i}_m,\vec{j}_n)b(z_i)$ ensures that the penalty is proportional to the strength of the H-bond. The dihedral angle ϕ_{kl} describes how the arm k of molecule i aligns with the arm l of molecule j along the vector joining the center of mass of these two molecules. Thus, the total dihedral energy between molecules i and j is

$$U_{\phi}(\vec{X}_i,\vec{X}_j)=\sum_{m,n}U^{mn}_{\phi}(\vec{X}_i,\vec{X}_j). \tag{10}$$

Note that because of the dependence on the local environment, $U^c_{\mathrm{HB}}(\vec{X}_i,\vec{X}_j)\neq U^c_{\mathrm{HB}}(\vec{X}_j,\vec{X}_i)$ and $U^{mn}_{\phi}(\vec{X}_i,\vec{X}_j)\neq U^{mn}_{\phi}(\vec{X}_j,\vec{X}_i)$. This asymmetry has no physical implications since U^c_{HB} and U_{ϕ} possess all the invariance properties required for a potential.[36]

We can now write the total potential energy between two water molecules as

$$E(\vec{X}_i,\vec{X}_j) = U_{\mathrm{LJ}}(r_{ij}) + U^c_{\mathrm{HB}}(\vec{X}_i,\vec{X}_j) + U_\phi(\vec{X}_i,\vec{X}_j). \quad (11)$$

This model has ten parameters which were chosen such as to account for a semiquantitative agreement of the density profile with experiment. We proceeded in two steps to adjust these parameters. First, we chose the values for these parameters such as to produce a density in g/cm^3 (Ref. 32) that is comparable to experimental values, i.e., about 1 g/cm^3 for the liquid phase and 0.95 g/cm^3 for the ice phase. Only under this condition can the structure of the model be qualitatively similar to real water. Then, we adjusted the parameters such as to obtain a density that is a concave function of temperature with its maximum close to the freezing point. This second condition is the minimal requirement for describing the anomalous properties of water.

The set of parameters calibrated according to the above procedure is given here in reduced units. We report energies and distances in terms of the binding energy $|\epsilon_{\mathrm{HB}}|$ and equilibrium distance R_{HB} of the H-bond. In these units, the three binding energies describing the system are $\epsilon_{\mathrm{HB}}=-1$, $\epsilon_{\mathrm{LJ}}=0.05$, and $\epsilon_\phi=0.01$. The two distances are $R_{\mathrm{HB}}=1$ and $\sigma_{\mathrm{LJ}}=1.04/2^{1/6}$. The two terms controlling H-bond interaction are $\sigma_R=0.1$ and $\sigma_\theta=0.08$, and the three parameters controlling the penalty of crowded environments are $\upsilon=0.5$, $R=1.3$, and $D=0.2$. In this work, temperature is given in units of $|\epsilon_{\mathrm{HB}}|/k_B$, where Boltzmann's constant k_B is set to unity. Pressure is given in units of $|\epsilon_{\mathrm{HB}}|/R^3_{\mathrm{HB}}$.

While adjusting the parameters, we found that the behavior of the system is robust upon changing the variables characterizing crowded environments. It is, however, sensitive to the ratio between the binding energy of the van der Waals interaction and the binding energy of the H-bond. This ratio controls the interplay of forces leading to an environment where MB molecules are radially surrounded by their first neighbors, and forces favoring a tetrahedral distribution of the first neighbors. The latter favors a high density configuration while the former accounts for a low density one. As opposed to the 2D MB model, we kept the equilibrium distance of the van der Waals interaction comparable to the equilibrium distance of the H-bond such as to avoid artificial peaks in the RDF.[31]

C. Numerical simulation method

For numerical simulations, we use the isothermal-isobaric (*NPT*) ensemble to study the thermodynamical properties of a system made of $N=256$ MB particles.[37] A Monte Carlo scheme is used where, at each step, an attempt is made to displace the center of mass and the orientation of particles randomly by a quantity $\Delta R_{\max}$ and 0.125 rad, respectively. The maximum translational displacement is chosen such as to give an acceptance ratio of 50%. Periodic boundary conditions are used to mimic an infinite system and at every 5 Monte Carlo sweeps, an attempt to rescale the size of the box is made (1 Monte Carlo sweep is equivalent to N attempted steps).

To obtain thermodynamical data throughout the desired range of temperatures, the initial configuration of the system is chosen randomly and equilibrated at the highest temperature ($T=0.17$) for 5×10^4 sweeps, after which statistics are gathered for the same amount of time. Then, the system is cooled down by $\Delta T=0.002$ and a similar cycle of equilibration/data gathering is performed. Close to the freezing temperature ($T<0.132$) equilibration/data gathering were performed for much longer times: 1.5×10^5 sweeps. This cooling procedure is repeated until the lowest temperature, i.e., $T=0.11$ is reached. At the transition temperature additional cycles of equilibration/statistics gathering ensured that the system was equilibrated properly. For all the pressures studied here, this protocol was repeated for ten samples differing by the initial condition. All the quantities reported are the average over those ten samples and, whenever relevant, the root-mean-square of this average is also shown as the error bar.

The quantities computed during the simulations were the average potential energy per particle E, the volume per particle V, the heat capacity C_P, the compressibility κ_T, and the thermal expansion coefficient α_P. The last three quantities are computed mathematically from the standard fluctuation relations:

$$C^*_P = \frac{C_P}{k_B} = \frac{\langle H^2\rangle - \langle H\rangle^2}{NT^2},$$

$$\kappa^*_T = \frac{\langle V^2\rangle - \langle V\rangle^2}{T\langle V\rangle}, \quad (12)$$

$$\alpha^*_P = \frac{\langle VH\rangle - \langle V\rangle\langle H\rangle}{T^2\langle V\rangle},$$

where H corresponds to the enthalpy of the system. As for the other quantities computed during the simulation, these response functions will be given in reduced units. Thus, C^*_P will be reported in dimensionless units, κ^*_T in terms of $R^3_{\mathrm{HB}}/\epsilon_{\mathrm{HB}}$ and α^*_P in units of $\epsilon^{-1}_{\mathrm{HB}}$.

III. RESULTS

In Fig. 3, we provide a qualitative comparison between the properties of bulk water (left panels) and the MB model at $P=0.2$ (right panels). The behavior of the MB model follows the trends of water quite accurately: The anomalous density profile (panels on the first row), the negative thermal expansivity (second row), the minimum in the isothermal compressibility (third row), and the large heat capacity (fourth row).

At ambient pressure, water freezes into an open-packed configuration called hexagonal-ice, i.e., Ice-I_h. This structure is held together by H-bonds which break when ice melts. At this transition, water molecules fill part of the empty spaces, assuming a higher density. In the liquid phase close to the melting temperature, a few open-packed configurations persist—held together by H-bonds. As the system is heated up, those bonds melt gradually removing empty spaces and increasing the density of the system. This reduction in empty spaces occurs until the temperature of maximum density is reached. Beyond this point thermal fluctuations decrease the density of the system with increasing temperature. This behavior has been measured experimentally [Fig. 3(a)] and is captured by the MB model [Fig. 3(b)]: Abrupt increase in the

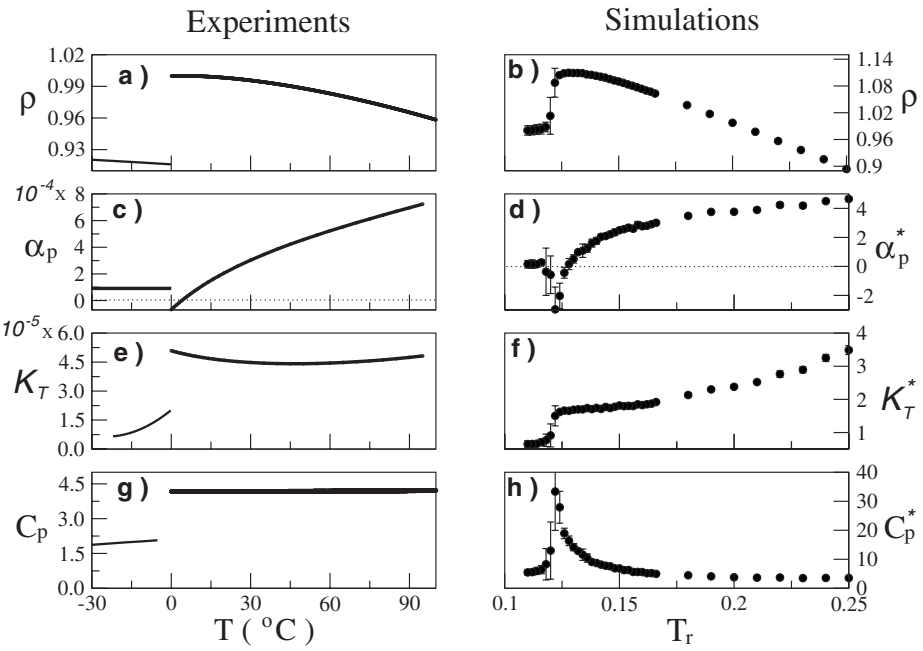

FIG. 3. Thermodynamical properties of water. Left: Experiments—data obtained from Ref. 38. Units are ρ (g/cm^3), α_P (K^{-1}), C_P (J/g K), and κ_T (bar^{-1}). Right: Simulations. Units are α_P^* (ϵ_{HB}^{-1}), κ_T^* (R_{HB}^3/ϵ_{HB}), and C_P^* (dimensionless units).

density at the melting transition and concave temperature dependence for the density of water with a maximum close to the melting transition.

The thermal expansion coefficient is proportional to the derivative of the volume with respect to temperature $\alpha_P = 1/V(\partial V/\partial T)_P$. As for most materials, α_P is positive and decreases upon cooling [Fig. 3(c)]—indicating that at high temperatures, the volume of water decreases with temperature. It becomes zero at the temperature of maximum density and negative close to the freezing point. This unusual negative expansivity is reproduced in the model [Fig. 3(d)] and reflects the unusual behavior of water to expand upon cooling below the temperature of maximum density.

The isothermal compressibility measures the tendency of a system to change its volume when the applied pressure is varied: $\kappa_T = -1/V(\partial V/\partial P)_T$. For a typical material, κ_T decreases upon cooling since it is related to density fluctuations whose amplitude becomes smaller as temperature decreases. This is in contrast with the behavior of water [Fig. 3(e)]. The compressibility of water is a convex function of temperature and has a minimum. This anomalous behavior can be explained by noticing that the compressibility is lower for highly packed system than for loosely packed ones since highly packed systems are less susceptible to rearrange their conformation when subjected to a pressure change. Thus, κ_T correlates with the volume of the system.[19] Now, since the volume of water is a convex function of temperature, κ_T is also convex with respect to temperature—see Fig. 3(e). Figure 3(f) shows that the simulated compressibility is also a convex function of temperature, although the curvature is not very pronounced and its minimum is not as pronounced as in experiments.

Heat capacity, which measures the capacity of a system to store thermal energy ($C_P = (dH/dT)_P$), is much higher in water than in ice—see Fig. 3(g). This has been explained by the multiple energy storage mechanisms of water as the breakage of van der Waals interactions and H-bonds. The heat capacity of the model presents a much higher variability than real water: Close to the transition, C_P is much higher than ice and this quantity decreases fast, reaching the same value as ice at about $T=0.15$.

In Fig. 4(a), we illustrate schematically the coexistence lines of the solid, liquid, and vapor phases of a simple material. At any point along those lines, the free energies of the adjacent phases are equivalent and the Clausius–Clapeyron equation is obtained by equating them:

$$\left(\frac{dP}{dT}\right)_{\text{coex}} = \frac{\Delta h}{T\Delta v}. \tag{13}$$

Since $\Delta h < 0$ and $\Delta v < 0$ for the liquid to solid transition of typical materials, $(dP/dT)_{\text{coex}}$ is positive. As a result of this positive slope, a typical liquid freezes when pressure is applied to it—as illustrated by the arrow on Fig. 4(a). On the other side, since water expands upon freezing, $\Delta v > 0$ while

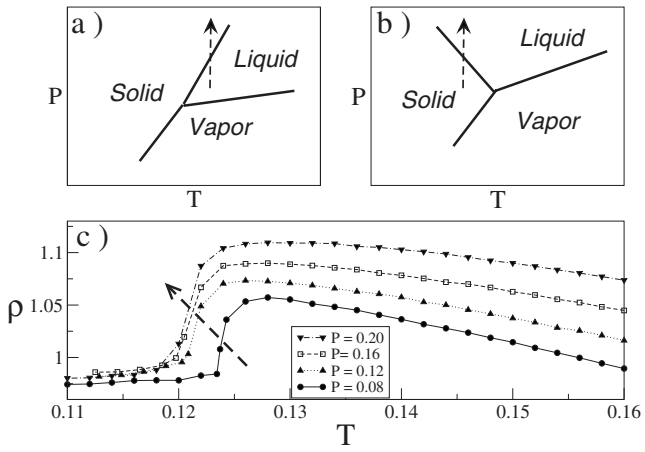

FIG. 4. Schematical representation of the phase diagram of a simple one-component substance (a) and water (b). The arrows indicate that pressure freezes a typical liquid but pressure melts ice. (c) Simulated density of the model for different values of pressure. The arrow indicates the shift of the freezing temperature to lower values as pressure increases.

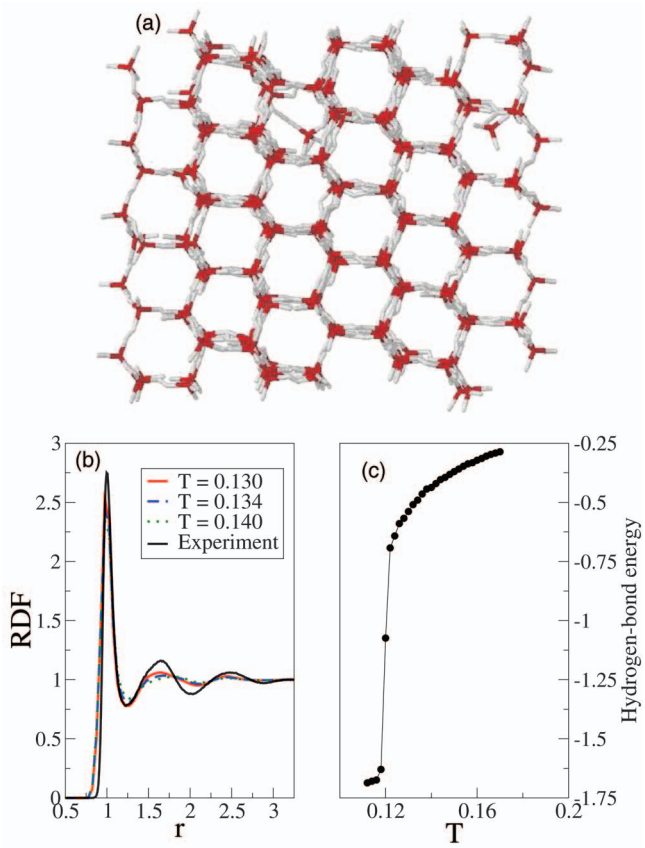

FIG. 5. (a) Ground state of the model: Ice-I_c. (b) Radial distribution function of the model at different temperatures compared to experimental data of water at 298 K. (c) Hydrogen-bond energy per water molecules as a function of temperature.

the enthalpy difference remains negative (ice has a lower enthalpy compared to water). Thus the coexistence line of the liquid-solid transition has a negative slope, i.e., $(dP/dT)_{\text{coex}}<0$. This is illustrated in Fig. 4(b) and leads to the melting of ice when pressure is applied to it. In Fig. 4(c) we show that the model reproduces this anomalous behavior of water. The simulated dependence of the density on temperature is shown for different values of pressure. The freezing temperature shifts to lower values as pressure increases, implying $(dP/dT)_{\text{coex}}<0$.

Figure 5(a) shows the structure obtained by freezing the MB model at $P=0.20$. This configuration corresponds to cubic Ice-I, i.e., Ice-I_c. Note that without a penalty term [Eq. (6)] the empty spaces found in Ice-I can be the stage for the formation of another tetrahedral-like lattice. Thus, this term efficiently shifts the energy of those compact configurations and, in particular, Ice-VII, in favor of Ice-I. In Fig. 5(b), the experimental RDF (Ref. 7) is compared to the ones of the model at different temperatures. The second peak of the RDF, commonly referred to as tetrahedral peak,[39] is a fingerprint of the tetrahedral geometry of water. It occurs at a distance given by the cosine rule, $d^2=2R_{\text{HB}}^2-2R_{\text{HB}}\cos(109.4°)\approx 1.6$, much smaller than for a simple liquid.[39] When compared to experiment, the model's RDF has slightly less structure but it peaks at the same position as the experiment—indicating that the average structure of the model agrees well with the experiment. In Fig. 5(c) we show the average energy of H-bonds per water molecule. Note that the H-bond energy of a water molecule making four perfect bonds is -2.0 (in units of ϵ_{HB}). In Fig. 5(c), the solid phase is very close to forming four perfect bonds: Its energy is ~ -1.73. On the other hand the energy of H-bonds in the liquid phase is much higher, i.e., between -0.25 and -0.75. This shows clearly that the four H-bonds of a MB molecule are distorted and therefore have a much higher energy than a perfect bond.

IV. CONCLUSION

In this work, we have constructed a simple but realistic model for water based on the MB approach.[19] At low temperature the model freezes forming Ice-I and it reproduces the main peaks of the experimental RDF of bulk water. In addition to these structural properties, the model reproduces the density anomaly of water: Ice has a lower density than water and the density of water is a concave function of temperature, with a maximum close to the freezing point. Also, the slope of the solid-liquid coexistence curve is found to be negative, in agreement with experiments.

In the 2D MB model, the H-bond interaction favors environments having three first neighbors at a distance R_{HB} which competes with the van der Waals interaction that favors six neighbors at a distance $0.7R_{\text{HB}}$. This competition is the underlying physics of the model that accounts for the density anomaly of bulk water. In the 3D MB model, H-bond and van der Waals interactions have the same equilibrium distance and the density anomaly results from an energy penalty for crowded environments. Without this penalty, the system would solidify into a compact Ice-VII configuration. With the penalty term, Ice-VII conformations compete with an open-packed diamondlike structure. The competition between these interactions is the underlying mechanism that leads to the density anomaly of the system.

The MB model for water is based on local interactions which are much faster to compute than other models that use long-range Coulomb forces. The drawback of local interactions is that the model cannot be used in studies involving charges or polarization effects. We believe that this model will provide new insights into water mechanisms related to molecular hydration. In particular, investigations of the hydrophobic effect are being undertaken with this model.

ACKNOWLEDGMENTS

C.L.D. would like to thank Razvan Nistor and Marco Aurelio Alves Barbosa for insightful discussions. He would also like to thank Alvarro Ferraz Filho and Silvio Quezado for kindly hosting his stay at the International Centre of Condensed Matter Physics (ICCMP) in Brasilia, Brazil, where part of this work was completed. We would like to thank SharcNet (www.sharcnet.ca) for computing resources. M.K. has been supported by the NSERC of Canada and T.A-N. by the Academy of Finland through its COMP CoE and TransPoly grants.

[1] M. Chaplin, Nat. Rev. Mol. Cell Biol. **7**, 861 (2006).
[2] W. L. Jorgensen, J. Chandrasekhar, J. D. Madura, R. W. Impey, and M. L. Klein, J. Chem. Phys. **79**, 926 (1983).

[3] I. Nezbeda, J. Mol. Liq. **73–74**, 317 (1997).
[4] B. Guillot, J. Mol. Liq. **101**, 219 (2002).
[5] C. Vega, J. L. F. Abascal, M. M. Conde, and J. L. Aragones, Faraday Discuss. **141**, 251 (2009).
[6] J. M. Sorenson, G. Hura, R. M. Glaeser, and T. Head-Gordon, J. Chem. Phys. **113**, 9149 (2000).
[7] A. K. Soper, Chem. Phys. **258**, 121 (2000).
[8] M. W. Mahoney and W. L. Jorgensen, J. Chem. Phys. **112**, 8910 (2000).
[9] H. J. C. Berendsen, J. P. M. Postma, W. F. van Gunsteren, and J. Hermans, in *Intermolecular Forces*, edited by B. Pullman (Reidel, Dordretch, 1981), p. 331.
[10] E. Neria, S. Fischer, and M. Karplus, J. Chem. Phys. **105**, 1902 (1996).
[11] D. J. Price and C. L. Brooks, J. Chem. Phys. **121**, 10096 (2004).
[12] H. W. Horn, W. C. Swope, J. W. Pitera, J. D. Madura, T. J. Dick, G. L. Hura, and T. Head-Gordon, J. Chem. Phys. **120**, 9665 (2004).
[13] Y. Wu, H. L. Tepper, and G. A. Voth, J. Chem. Phys. **124**, 24503 (2006).
[14] A. Baranyai and A. Bartók, J. Chem. Phys. **126**, 184508 (2007).
[15] V. Molinero and E. B. Moore, J. Phys. Chem. B **113**, 4008 (2009).
[16] M. A. A. Barbosa and V. B. Henriques, Phys. Rev. E **77**, 051204 (2008).
[17] C. Buzano, E. De Stefanis, A. Pelizzola, and M. Pretti, Phys. Rev. E **69**, 061502 (2004).
[18] M. Pretti and C. Buzano, J. Chem. Phys. **123**, 024506 (2005).
[19] K. A. T. Silverstein, A. D. J. Haymet, and K. A. Dill, J. Am. Chem. Soc. **120**, 3166 (1998).
[20] P. H. Poole, F. Sciortino, T. Grande, H. E. Stanley, and C. A. Angell, Phys. Rev. Lett. **73**, 1632 (1994).
[21] A. P. Lyubartsev and A. Laaksonen, Chem. Phys. Lett. **325**, 15 (2000).
[22] A. P. Lyubartsev, M. Karttunen, I. Vattulainen, and A. Laaksonen, Soft Mater. **1**, 121 (2002).
[23] W. Kauzmann, Adv. Protein Chem. **14**, 1 (1959).
[24] K. A. Dill, Biochemistry **29**, 7133 (1990).
[25] A. Ben-Naim, J. Chem. Phys. **54**, 3682 (1971).
[26] N. T. Southall and K. A. Dill, Biophys. Chem. **101–102**, 295 (2002).
[27] K. A. Dill, T. M. Truskett, V. Vlachy, and B. Hribar-Lee, Annu. Rev. Biophys. Biomol. Struct. **34**, 173 (2005).
[28] C. L. Dias, T. Ala-Nissila, M. Karttunen, I. Vattulainen, and M. Grant, Phys. Rev. Lett. **100**, 118101 (2008).
[29] J.-P. Becker and O. Collet, J. Mol. Struct.: THEOCHEM **774**, 23 (2006).
[30] A. Ben-Naim, *Water and Aqueous Solutions* (Plenum, New York, 1974).
[31] A. Bizjak, T. Urbic, V. Vlachy, and K. A. Dill, Acta Chim. Slov. **54**, 532 (2007).
[32] The density can be computed in g per cm^3 by mapping R_{HB} to its experimental value (Ref. 7), i.e., $R_{\mathrm{HB}}=2.78$ Å, and using $M=2.992\times10^{-23}$ g for the molecular mass of water: $\rho=(256/V)1.454\ 48$ g/cm^3.
[33] C. J. Roberts and P. G. Debenedetti, J. Chem. Phys. **105**, 658 (1996).
[34] G. M. Bell, J. Phys. C **5**, 889 (1972).
[35] J. D. Bernal and R. H. Fowler, J. Chem. Phys. **1**, 515 (1933).
[36] J. Tersoff, Phys. Rev. B **37**, 6991 (1988).
[37] We note that in the present study we have not carried out a systematic study of finite-size (FS) effects. Freezing is a first-order transition where we expect FS effects to be relatively weak [see, e.g., J. Lee and J. M. Kosterlitz, Phys. Rev. B **43**, 3265 (1991)].
[38] G. S. Kell, J. Chem. Eng. Data **20**, 97 (1975).
[39] J. L. Finney, J. Mol. Liq. **90**, 303 (2001).